JOC Article
pubs.acs.org/joc

Fluorescence Properties of Simple N-Substituted Aldimines with a B−N Interaction and Their Fluorescence Quenching by a Cyanide Ion

Junro Yoshino, Naokazu Kano,* and Takayuki Kawashima*

Department of Chemistry, Graduate School of Science, The University of Tokyo, 7-3-1 Hongo, Bunkyo-ku, Tokyo 113-0033, Japan

takayuki@chem.s.u-tokyo.ac.jp

Received August 10, 2009

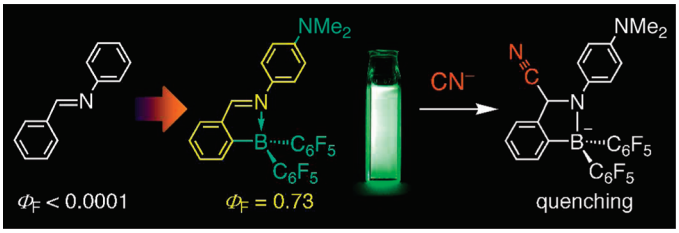

N-Aryl, *N*-alkyl, *N*-alkoxy, and *N*-amino derivatives of 2-[bis(pentafluorophenyl)boryl]benzylideneamine were synthesized by the condensation reactions of 2-[bis(pentafluorophenyl)boryl]-benzaldehyde with the corresponding amines. Their structures were investigated by NMR and X-ray crystallographic analysis. Their properties were investigated by UV−vis and fluorescence spectroscopy. The boryl-substituted *N*-arylimines show blue or green fluorescence in hexane at room temperature, and their fluorescence efficiency is much higher than that of *N*-benzylideneaniline. In particular, the boryl-substituted *N*-(4-dimethylaminophenyl)imine showed strong green emissions with at least 7000 times higher fluorescence quantum yield (0.73) compared with that of *N*-benzylideneaniline. The boryl-substituted *N*-(1-indolyl)- and *N*-(9-carbazolyl)imines showed dual emissions, one of which was assignable as arising from the lowest singlet excited state and the other from the local excited state of the substituent on the imine nitrogen. The fluorescent properties of the boryl-substituted *N*-butyl- and *N*-methoxyimines were also investigated. Reactions of the *N*-arylimine derivatives with cyanide ion gave the corresponding cyanide adducts and quenched the fluorescence, indicating that these 2-[bis(pentafluorophenyl)boryl]benzylideneamine derivatives have a potential as a cyanide ion sensor.

Introduction

Imine derivatives have been widely used as coloring materials and functional molecular units.[1] Imine derivatives can be synthesized readily by condensation reactions of aldehydes with amine derivatives. The two parts of the π-conjugated systems in an imine that is formed from aromatic aldehydes and aromatic amine derivatives can be connected through the π-orbital of the C=N double bond. These structures constructed by a simple synthetic method can provide highly diverse π-conjugated systems. Although such high diversity of their structures may provide a big advantage as fluorescence materials, imines are essentially nonfluorescent compounds. For example, the fluorescence quantum yield of *N*-benzylideneaniline is less than 10^{-4}.[2] Although several highly fluorescent imines bearing a metal−nitrogen interaction have been reported,[3] most of them required tri- or higher-dentate ligand structures (Figure 1). A restriction of their molecular designs to make their structures rigid results in difficulty in further modification of their structures to tune their fluorescence properties. In simpler imines, some salicylideneamine derivatives bearing an *O*,*N*-bidentate ligand structure have been reported as fluorescent imines. However, most of their fluorescence quantum

(1) Yamamoto, K.; Higuchi, M.; Shiki, S.; Tsuruta, M.; Chiba, H. *Nature* **2002**, *415*, 509.

(2) Belletete, M.; Durocher, G. *Can. J. Chem.* **1982**, *60*, 2332.

(3) (a) Morishige, K. *J. Inorg. Nucl. Chem.* **1978**, *40*, 843. (b) Hamada, Y.; Sano, T.; Fujita, M.; Fujii, T.; Nishio, Y.; Shibata, K. *Jpn. J. Appl. Phys.* **1993**, *32*, L511. (c) Wang, P.; Hong, Z.; Xie, Z.; Tong, S.; Wong, O.; Lee, C.-S.; Wong, N.; Hung, L.; Lee, S. *Chem. Commun.* **2003**, 1664.

Published on Web 09/01/2009 DOI: 10.1021/jo901733b

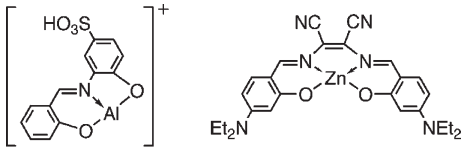

FIGURE 1. Previously reported highly fluorescent imines.

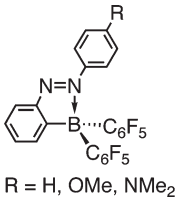

FIGURE 2. Fluorescent 2-borylazobenzenes.

yields are low. There are some fluorescent simple imines bearing a B−N interaction, but there have been only a few examples, and their fluorescence properties have scarcely been shown[4] except for those C=N double-bond compounds whose C=N double bond consists of part of a heterocycle.[5] Therefore, the relationship between structures and fluorescence properties of the boron-substituted imines is still unclear. Development of new methods to provide imines with fluorescence by simple modification should bring high flexibility to the molecular designs, make their fluorescence properties more diverse, and increase their usefulness as easily synthesizable and tunable fluorescent materials.

We recently reported the synthesis of fluorescent boron-substituted azobenzenes (Figure 2)[6] in the continuation of our work on 2-borylazobenzene derivatives.[7] Taking into consideration the similarity in structures between imines and azobenzenes, the simple introduction of a diarylboryl group to benzylideneamines was expected to provide a new class of fluorescent imines with a B−N interaction (Scheme 1). Direct introduction of a boryl group to the phenylimine π-conjugated system is considered to affect the system much more than its introduction through an oxygen atom in the case of salicylideneamine derivatives. Here, we report the synthesis of 2-(diarylboryl)phenylimine derivatives, the relationship between their structures and fluorescence, and their reactivities.

Results and Discussion

Synthesis of 2-Borylphenyl-Substituted Imines. Successive reactions of 2-bromobenzaldehyde diethyl acetal **1** with *n*-butyllithium and ethoxyborane **2** followed by hydrolysis under acidic conditions gave 2-borylbenzaldehyde **3** in 50% yield. 2-Borylphenyl-substituted imines **4a**−**c** and

SCHEME 1. New Design for Boron-Substituted Imine Derivatives

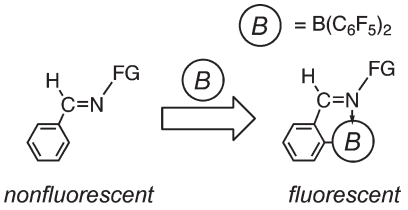

5−**9** were synthesized by dehydrative condensation of **3** and the corresponding amines in good to moderate yields (Scheme 2 and Table 1).

Structures. X-ray crystallographic analyses were performed for **4a**−**c** and **5**−**9**, and their crystal structures are shown in Figures S1−S3 in Supporting Information. In hydrazone **8**, there are two independent molecules of **8** in the unit cell, having almost identical structures. There is an intramolecular coordination from the imine nitrogen to the boron in all cases in the crystalline state. The bond lengths of the coordination bonds shown in Table 2 [1.60−1.65 Å] are close to the sum of the covalent radii of boron and nitrogen (1.57 Å), indicating the strong B−N interactions in **4a**−**c** and **5**−**9**. Their imine C−N bond lengths [1.29−1.30 Å] are slightly longer than the C=N double bond length of *N*-benzylideneaniline (**10**) (1.276(1) Å),[8] and much shorter than the usual C−N single bond lengths (1.38 Å), indicating that the imine C−N bonds in **4a**−**c** and **5**−**9** maintain their double-bond character. In anthrylimine **6**, an anthryl group and a C_6F_5 group of another molecule are stacked intermolecularly. In hydrazone **8**, intramolecular $\pi-\pi$ stacking between the indolyl group and one of the C_6F_5 groups (Figure S2, Supporting Information) and intermolecular $\pi-\pi$ stackings between two neighboring indolyl groups, two C_6F_5 groups, or the indolyl group and one of the C_6F_5 groups are found (see Supporting Information). In hydrazone **9**, there is only intramolecular $\pi-\pi$ stacking between the carbazolyl group and a C_6F_5 group (Figure S2, Supporting Information). Compounds **4a**−**c**, **5**, and **7** have neither intermolecular nor intramolecular stacking. The existence of the intramolecular B−N interactions is unaffected by whether the $\pi-\pi$ stackings exist or not. The ^{11}B NMR chemical shifts of 2-borylphenyl-substituted imines **4a**−**c** and **5**−**9** in $CDCl_3$ were observed between −3.2 and −0.6 ppm, showing the tetracoordination state of the boron atoms in solution as in the crystal structures.

The C=N double-bond planes of hydrazones **8** and **9** are approximately perpendicular to their nitrogen-containing heterocycles, probably because of the aforementioned intramolecular $\pi-\pi$ stackings. The indolyl and carbazolyl groups are almost parallel to one of the C_6F_5 groups, and their benzene rings are overlapped with the C_6F_5 group. In contrast, imines **4a**−**c** and **5**−**7** have a relatively planar *N*-substituted phenylimine moiety, judging from the torsion angles ω_1 [torsion angle between C7−N1−X−Y; **4a**−**c**, **5**, and **6**: (X, Y) = (C8, C9), **7**: (X, Y) = (O1, C8), **8** and **9**: (X, Y) = (N2, C8)] and ω_2 [torsion angle between C1−C6−C7−N1] shown in Table 2.

(4) (a) Padmanathan, T. DE1926925, **1970**. (b) Allmann, R.; Hohaus, E.; Olejnik, S. *Z. Naturforsch.* **1982**, *37B*, 1450. (c) Mir, J. M.; Martinez, C. *Talanta* **1986**, *33*, 541. (d) Riddle, J. A.; Lathrop, S. P.; Bollinger, J. C.; Lee, D. *J. Am. Chem. Soc.* **2006**, *128*, 10986.

(5) (a) Wakamiya, A.; Taniguchi, T.; Yamaguchi, S. *Angew. Chem., Int. Ed.* **2006**, *45*, 3170. (b) Son, H.-J.; Han, W.-S.; Wee, K.-R.; Chun, J.-Y.; Choi, K.-B.; Han, S.-J.; Kwon, S.-N.; Ko, J.; Lee, C.; Kang, S. O. *Eur. J. Inorg. Chem.* **2009**, 1503.

(6) (a) Yoshino, J.; Kano, N.; Kawashima, T. *Chem. Commun.* **2007**, 559. (b) Yoshino, J.; Kano, N.; Kawashima, T. *Chem. Lett.* **2008**, *37*, 960.

(7) (a) Kano, N.; Yoshino, J.; Kawashima, T. *Org. Lett.* **2005**, *7*, 3909. (b) Yoshino, J.; Kano, N.; Kawashima, T. *Tetrahedron* **2008**, *64*, 7774.

(8) Harada, J.; Harakawa, M.; Ogawa, K. *Acta Crystallogr. B* **2004**, *60*, 578.

SCHEME 2. Synthesis of 4a−c and 5−9 via 3 and Structural Formula of *N*-Benzylideneaniline (10)

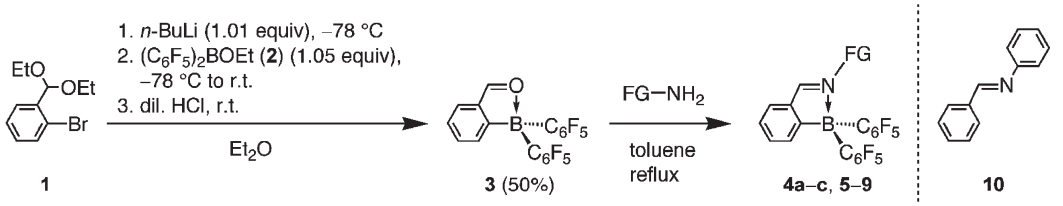

TABLE 1. Yields of 2-Borylphenyl-Substituted Imines 4a−c and 5−9

entry	FG	product	yield/%
1		**4a**	83
2		**4b**	55
3	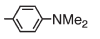	**4c**	86
4	*n*-Bu	**5**	93
5	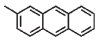	**6**	100
6[a]	OMe	**7**	67
7		**8**	100
8[b]		**9**	100

[a]$MeONH_2 \cdot HCl$, EtOH, pyridine, rt. [b]Et_2O, rt.

TABLE 2. Selected Bond Lengths (*d*) and Torsion Angles (ω) of Imines 4a−c and 5−9

compound	d_1(B−N), Å	d_2(C−N), Å	ω_1[a], deg	ω_2[b], deg
4a	1.619(2)	1.294(2)	25.6(2)	4.05(18)
4b	1.6222(18)	1.2981(17)	13.66(18)	1.23(15)
4c	1.6160(18)	1.3003(18)	28.96(19)	2.87(16)
5	1.602(3)	1.287(2)	17.0(3)	1.2(2)
6	1.620(4)	1.294(3)	33.5(4)	2.8(4)
7	1.605(3)	1.285(3)	5.7(3)	1.2(2)
8[c]	1.6132(19)	1.2952(18)	61.73(18)	3.72(17)
	[1.618(2)]	[1.2948(18)]	[72.88(17)]	[4.71(17)]
9	1.646(3)	1.295(2)	72.0(2)	5.8(2)

[a]Torsion angle between C7−N1−X−Y. **4a−c**, **5**, and **6**: (X, Y) = (C8, C9). **7**: (X, Y) = (O1, C8). **8** and **9**: (X, Y) = (N2, C8). [b]Torsion angle between C1−C6−C7−N1. [c]Values for another independent molecule are in brackets.

Absorption and Fluorescence Properties of *N*-Alkyl- and *N*-Arylimines. In the UV−vis absorption spectra in hexane, imines **4a−c**, **5**, and **6** showed a strong absorption in the UV region, as shown in Table 3 and Figure 3. These absorption maxima are assignable to the $\pi-\pi^*$ transition of the imine moiety. The wavelengths of the $\pi-\pi^*$ absorption maxima of *N*-phenylimine **4a**, *N*-butylimine **5**, and *N*-anthrylimine **6** become longer in the order of **5** < **4a** < **6**, reflecting the extension of the π-conjugation. In the cases of **4a−c**, the electron-donating groups in the π-conjugated systems also effectively produced a red shift of the absorption maxima.

Fluorescence spectra and fluorescence properties of **4a−c**, **5**, and **6** are shown in Figure 4 and Table 3, respectively. Imine **4a** showed blue emission in hexane at rt upon UV irradiation (Figure 5A). In the fluorescence spectrum, imine **4a** showed an emission maximum at 460 nm and the fluorescence quantum yield was determined to be 0.0050, which is a higher fluorescence efficiency than nonfluorescent *N*-benzylideneaniline (**10**) (Φ_F < 0.0001).[9] Imines bearing a more extended π-conjugated system and/or an electron-donating aryl group on the nitrogen atom showed fluorescence that was more red-shifted with higher fluorescence efficiency. For example, *N*-[4-(dimethylamino)phenyl]imine **4c** and *N*-anthrylimine **6** showed strong green emission (Figure 5B) with fluorescence quantum yields (0.73 and 0.39, respectively) very much higher than that of *N*-benzylideneaniline (**10**). It is considered that introduction of the bis(pentafluorophenyl)-boryl group and the eventual B−N interaction played important roles in providing imines **4a−c** and **6** with such

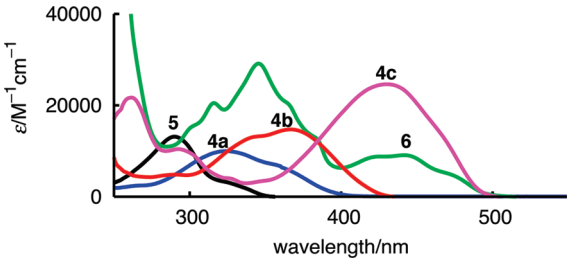

FIGURE 3. UV−vis absorption spectra of imines **4a−c**, **5**, and **6** in hexane.

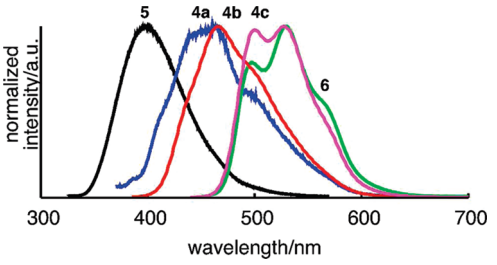

FIGURE 4. Fluorescence spectra of imines **4a−c**, **5**, and **6** in hexane.

high fluorescence efficiencies. These increased fluorescence quantum yields would be caused by suppression of nonradiative relaxation of the excited state by increasing the rigidity of the molecular structure with a tight B−N bond and a rigid five-membered ring framework. An electron-donating group at the end of the imine π-conjugated system, such as dimethylamino group of **4c**, is also considered to contribute to increasing the rigidity of the molecular structure by planarization of the diarylimine moiety due to the delocalization of the lone pair to the imine π-conjugated system. Furthermore, masking of the lone pair of the

(9) Belletete, M.; Durocher, G. *Can. J. Chem.* **1982**, *60*, 2332.

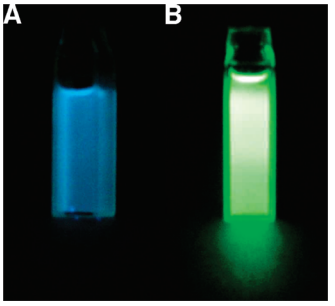

FIGURE 5. Photographs of (A) **4a** and (B) **6** in hexane upon UV irradiation.

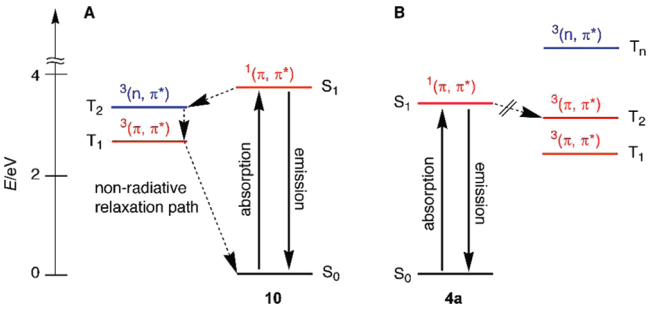

FIGURE 6. Calculated energy levels of singlet and triplet excited states of (A) **10** and (B) **4a** at the B3PW91/6-31+G(d) level of theory. The ^{3}(n, π*) state of **4a** was not detected between T_1 and T_{12} (4.2 eV).

nitrogen atom by coordination to the boron atom is considered to contribute to removing the factors for the absence of fluorescence in **10**, that is, the high rate of nonradiative relaxation process with the intersystem crossing from the lowest singlet excited state to triplet excited states[10] and the existence of a lone pair spatially perpendicular to the π-orbitals, which undergoes rapid intersystem crossing.

To clarify this point, theoretical calculations using DFT and time-dependent DFT (TD-DFT) methods at the B3PW91/6-31+G(d) level of theory were performed. Optimized structures of **4a** and **7**−**10** and energy levels of their molecular orbitals were obtained by the DFT calculations. The energy levels of their singlet and triplet excited states and identification of each excitation were obtained by the TD-DFT calculations. In *N*-benzylideneaniline (**10**), its two triplet excited states, T_1 (2.6 eV) and T_2 (3.3 eV), were at lower energy levels than the S_1 state (3.7 eV) (Figure 6A). Both the S_1 and T_1 states consist of an excitation from the HOMO to the LUMO. The T_2 state consists of an excitation from the HOMO−2 to the LUMO.[11] The LUMO (−1.9 eV), HOMO (−6.2 eV), and HOMO−2 (−7.2 eV) of **10** are mainly made up by the π*, π, and n orbitals of the azomethine group, respectively (Figure 7). Therefore, the S_1, T_1, and T_2 states should be $^1(\pi, \pi^*)$, $^3(\pi, \pi^*)$, and ^{3}(n, π*) excited states. The intersystem crossing $^1(\pi, \pi^*) \rightarrow {}^3$(n, π*) would be relatively fast because of the large spin−orbit interaction between the lone pair on the nitrogen atom and the π orbital

(10) Knyazhanskii, M,. I.; Stryukov, M. B.; Minkin, V. I. *Opt. Spectrosc.* **1972**, *33*, 484.

(11) The TD-DFT calculations indicate that the T_2 state also consists of an excitation from the HOMO−1 to the LUMO, but its contribution is smaller than that of the excitation from the HOMO−2.

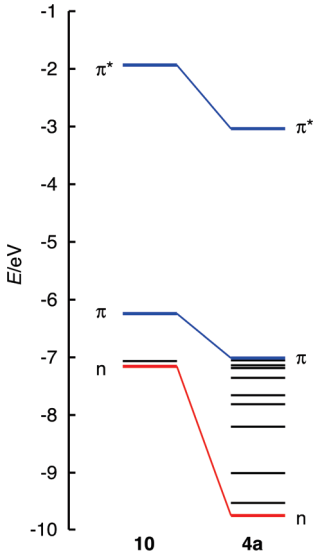

FIGURE 7. Calculated energy levels of frontier orbitals of **10** and **4a** at the B3PW91/6-31+G(d) level of theory.

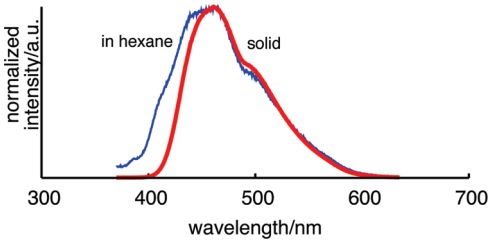

FIGURE 8. Fluorescence spectra of imine **4a** in the solid state (bold line) and in the solution state (thin line).

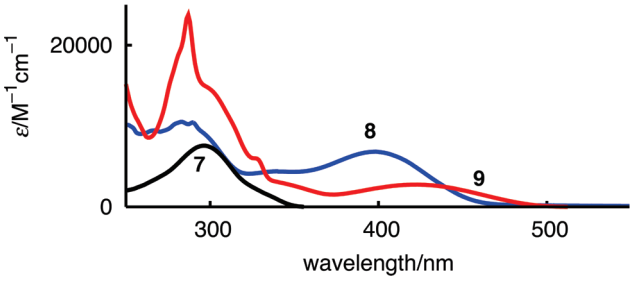

FIGURE 9. UV−vis absorption spectra of imines **7**−**9** in hexane.

perpendicular to it.[12] These high rates of the relaxation processes including the intersystem crossing process should effectively suppress the $S_1 \rightarrow S_0$ radiative relaxation process and cause the absence of fluorescence in **10**. In **4a**, there is a B−N dative bond, and the orbital formed from the bonding orbital between the N and B atoms and the π orbital of the C_6F_5 groups in **4a** is greatly stabilized by the B−N interaction and becomes HOMO−10 (−9.7 eV), while the π and π* orbitals of the imine moiety of **4a** become the HOMO (−7.0 eV) and the LUMO (−3.0 eV), respectively (Figure 7). Although two triplet excited states, T_1 (2.4 eV) and T_2 (3.1 eV), were at lower energy levels than the S_1 state

(12) El-Sayed, M. A. *J. Chem. Phys.* **1963**, *38*, 2834.

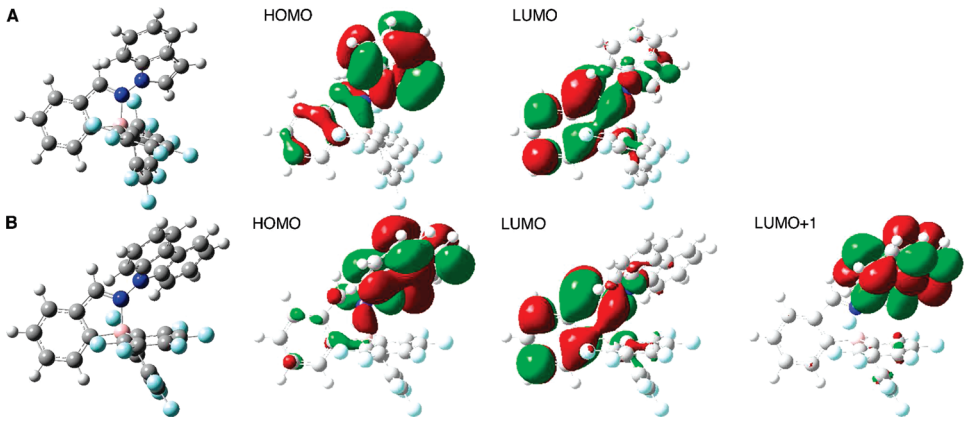

FIGURE 10. Molecular structures and molecular orbital diagrams for (A) **8** and (B) **9** calculated at the B3PW91/6-31+G(d) level of theory. Gray, white, pink, aqua, and blue balls in molecular structures indicate carbon, hydrogen, boron, fluorine, and nitrogen atoms, respectively.

(3.4 eV) for **4a**, neither the S_1, T_1, nor T_2 states had the character of the n$-\pi^*$ excited state (Figure 6B), because both S_1 and T_1 states consist of excitation from the HOMO to the LUMO and the T_2 state consists of excitation from the HOMO-5 (-7.6 eV), which is mainly made up by the π-orbital on the benzene ring of **4a**, to the LUMO. The S_1 state should be $^1(\pi, \pi^*)$ excited state. The T_1 and T_2 states should be $^3(\pi, \pi^*)$ excited states. As a result, the rate of the relaxation paths from excited **4a** including $S_1 \rightarrow T_2$ and/or $S_1 \rightarrow T_1$ intersystem crossings would be lower than those of **10**, so that the $S_1 \rightarrow S_0$ radiative relaxation process of **4a** can compete with its nonradiative relaxation processes. Therefore, this not-suppressed, allowed $\pi-\pi^*$ transition would provide **4a** with high emitting ability.

Compound **4a** also showed fluorescence in the solid state. A blue emission was observed upon UV irradiation. In the fluorescence spectra at room temperature, it showed an emission maximum at 461 nm (Figure 8). This emission wavelength is almost the same as that in hexane, indicating that intermolecular interaction of **4a** in the solid state is comparable with that in the solution state.

Absorption and Fluorescence Properties of an Oxime and Hydrazones. *N*-Methoxyimine **7** showed its absorption maximum at 296 nm in hexane (Figure 9). This blue shift of the absorption maximum from that of *N*-phenylimine **4a** (324 nm) is due to the existence of the oxygen lone pair, which is significantly conjugated with the π-orbitals of the benzylideneamine moiety. This contribution of the methoxy group in **7** makes its absorption blue-shifted by producing a higher energy level of the LUMO (-2.6 eV) compared with that of **4a** (-3.0 eV), while the HOMO energy levels of both **7** and **4a** were almost equal (-7.0 eV for each). In the fluorescence spectrum in hexane, **7** showed no fluorescence, in contrast to the aforementioned *N*-aryl and *N*-alkylimines, which showed fluorescence. This may also be an effect of the lone pair on the oxygen atom.

The UV$-$vis and fluorescence spectra of *N*-indolylimine **8** and *N*-carbazolylimine **9** in hexane showed a different aspect from the other imines described above. Their longest absorption maximum appeared as a broad peak at 398 and 423 nm, respectively (Figure 9), suggesting that the transition between the ground state and the lowest singlet excited state has a charge-transfer character. The molecular orbitals and the nature of the absorption of hydrazones **8** and **9** were

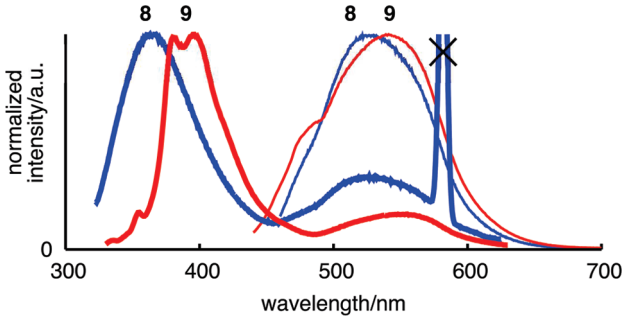

FIGURE 11. Fluorescence spectra of hydrazones **8** and **9** in hexane. Thin lines indicate spectra upon excitation at wavelengths of their absorption maxima (**8**, 398 nm; **9**, 423 nm), and bold lines indicate those upon excitation at shorter wavelengths (**8**, 290 nm; **9**, 320 nm). In the spectra of **8** upon irradiation at 290 nm, the spike-shaped peak at 580 nm (cross-marked) is not a part of fluorescence peak of **8** but the second-order scattering light.

investigated by DFT and TD-DFT calculations. The optimized structures of **8** and **9** match well with their crystal structures. The moderately perpendicular structures at their N$-$N bonds disconnect the conjugation between the π-orbitals of the substituent on the imine nitrogen and the benzylideneamine moiety. According to the TD-DFT calculations, the transitions between the ground state and the lowest singlet excited states of **8** and **9** were assignable to the transitions between the HOMOs and the LUMOs. Their HOMOs and LUMOs consist mainly of the π-orbitals of the substituent on the imine nitrogen and the benzylideneamine moiety, respectively (Figure 10). The transition between these spatially separated HOMOs and LUMOs would have charge-transfer character. Therefore, the charge-transfer character of the transitions for the longest absorption maxima of **8** and **9** suggest that the greatly twisted structures shown by the X-ray crystallographic analysis and the theoretical calculations were also dominant in the solution state.

In the fluorescence spectra in hexane, **8** and **9** showed a single emission with the emission maximum at 525 and 545 nm, respectively, as shown in Figure 11, upon excitation at wavelengths of their longest absorption maximum, 398 and 423 nm, respectively. In contrast, they showed dual emissions as shown in Table 3 and Figure 11 upon excitation at shorter wavelengths, 290 nm for **8** and 320 nm for **9**,

TABLE 3. Absorption Maxima (λ_{abs}), Molar Absorption Coefficients (ε), Fluorescence Wavelengths (λ_{em}), and Fluorescence Quantum Yields (Φ_F) of Imines 4a−c and 5−9 in Hexane at Room Temperature

compound	λ_{abs}, nm	ε, M^{-1} cm^{-1}	λ_{em}[a], nm	Φ_F[a]
4a	324	1.0×10^4	460	0.0050[b]
4b	366	1.5×10^4	466	0.074[b]
4c	439	2.5×10^4	500, 527	0.73[c]
5	290	1.3×10^4	398	0.011[b]
6	442	9.1×10^3	497, 531	0.39[c]
7	296	7.6×10^3	[d]	
8	398	6.8×10^3	525	0.0092[b]
			(365, 531)[e]	([f])[e]
9	423	2.7×10^3	545	0.0052[b]
			(380, 396, 545)[g]	(0.020)[b,g]

[a]Unless otherwise noted, excited at the longest absorption maxima. [b]Based on 9,10-diphenylanthracene in cyclohexane (Φ_F = 1.0). [c]Based on fluorescein in 0.1 M aq NaOH (Φ_F = 0.85). [d]No fluorescence. [e]Excited at 290 nm. [f]Not determined. [g]Excited at 320 nm.

suggesting that two radiative relaxation paths for **8** and **9** exist. In the cases of **8** and **9**, the wavelengths of the lowest energy emission bands upon excitation at both longer and shorter wavelengths are almost the same, indicating that they originate from the same excited states. Their excitation spectra for these emission bands matched with their absorption spectra, and the shapes of these emission bands consisted of the mirror images of the longest absorption peaks. Therefore, these lowest energy emission bands are considered to be emission from the lowest singlet excited states, those from the CT states. The excitation spectrum of **9** for the higher energy emissions (396 nm) showed maxima at 326 and 340 nm. The peak shapes of this higher energy emission and the corresponding absorption resemble those of the emission and absorption of carbazole. In addition, their emission and absorption wavelengths are close to each other (λ_{abs} of carbazole = 292 and 332 nm; λ_{em} of carbazole = 335 and 347 nm in cyclohexane at 298 K).[13] Judging from these observations, this higher energy emission of **9** is considered to be an emission from the local excited state of the carbazolyl moiety. Lifetimes of fluorescence of **9** for the emissions at 396 and 545 nm upon excitation at 320 nm were measured as 18.15(8) and 5.27(7) ns, respectively. A lifetime of fluorescence of **9** at 545 nm upon excitation at 395 nm was determined as 5.39(3) ns, and it was considered to be identical to that upon excitation at 320 nm. These two fluorescence lifetimes of **9** for the higher and the lower energy emissions were different but not so largely different. Fluorescence lifetimes of **8** showed the same tendency. The higher energy emission of **8** is considered to be an emission from the local excited state of the indolyl moiety by analogy with the case of **9**. In the TD-DFT calculations of **9**, the transition giving the local excited state of the substituent on the imine nitrogen was found as the transition between the HOMO and the LUMO+1 (Figure 10B). On the basis of these calculations, the dual fluorescence behavior of **9** is explained as shown in Scheme 3. First, UV irradiation at the absorption band of the carbazolyl moiety gives the local excited state of the carbazolyl moiety, consisting of the excitation from the HOMO to the LUMO+1. One fate of this excited state is the direct radiative relaxation to the ground state, giving the higher energy emission band. Another fate is relaxation to the lowest singlet excited state, formally consisting of the

(13) Bonesi, S. M.; Erra-Balsells, R. *J. Lumin.* **2001**, *93*, 51.

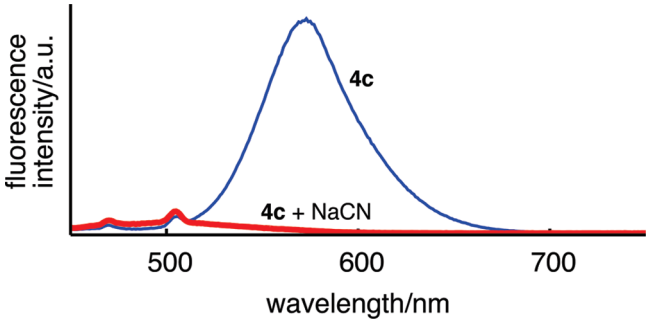

FIGURE 12. Fluorescence spectra of **4c** (4.1 μM) in DMF before (thin line) and after (bold line) addition of sodium cyanide.

excitation from the HOMO to the LUMO, and this process involves the intramolecular electron transfer from the substituent on the imine nitrogen to the benzylideneamine moiety of **9** (Scheme 3). Finally, emission from the S_1 state gives the lower energy emission band. The case of **8** is explained analogously.[14] The dependence of emission behavior on the excitation wavelength is explained as follows: excitation at short enough wavelengths gives the local excited states of the carbazolyl or indolyl moieties and produces dual emissions. In contrast, excitation at longer wavelengths only gives the lowest excited state and produces only single, low-energy emission. Therefore, the spatially separated π-orbitals of hydrazones **8** and **9**, which are the result of the moderately perpendicular structures, would provide them with the dual emission phenomenon.

Reaction of a Boron-Substituted Diphenylazomethine with a Cyanide Source. Imines are known to form the corresponding α-aminonitriles by addition of cyanide ion in the presence of a proton source, as represented by the Strecker reaction.[15] Aldimines, such as *N*-benzylideneaniline (**10**), are also known to give aldimine-coupling products via cyanide adducts at imine carbons.[16] Boron compounds also react with a cyanide ion, resulting in formation of cyanoborates.[17] These reactions of imines or boranes with a cyanide source would greatly change their optical properties. Because the fluorescent boron-substituted imines have two reactive sites for a cyanide ion, a C=N double bond and a boron center, both reactions are possible and are expected to change the fluorescence properties. To determine which site reacts with a cyanide ion, reactions of imines **4a** and **4c** with a cyanide ion were investigated. In the absorption spectra in DMF, the absorption maximum of **4c** (440 nm) completely disappeared after addition of excess sodium cyanide, and new absorption maxima (302 and 328 nm) appeared instead. This large blue

(14) The transition giving the local excited state of the substituent on the imine nitrogen in **8** was detected as the transition between the HOMO and the LUMO+2.

(15) Strecker, A. *Ann. Chem. Pharm.* **1850**, *75*, 27.

(16) (a) Walia, J. S.; Singh, J.; Chattha, M. S.; Satyanarayana, M. *Tetrahedron Lett.* **1969**, *10*, 195. (b) Walia, J. S.; Guillot, L.; Singh, J.; Chattha, M. S.; Satyanarayana, M. *J. Org. Chem.* **1972**, *37*, 135. (c) Reich, B. J. E.; Greenwald, E. E.; Justice, A. K.; Beckstead, B. T.; Reibenspies, J. H.; North, S. W.; Miller, S. A. *J. Org. Chem.* **2005**, *70*, 8409.

(17) (a) Badugu, R.; Lakowicz, J. R.; Geddes, C. D. *Anal. Biochem.* **2004**, *327*, 82. (b) Badugu, R.; Lakowicz, J. R.; Geddes, C. D. *Anal. Chim. Acta* **2004**, *522*, 9. (c) Badugu, R.; Lakowicz, J. R.; Geddes, C. D. *Dyes Pigm.* **2005**, *64*, 49. (d) Badugu, R.; Lakowicz, J. R.; Geddes, C. D. *J. Am. Chem. Soc.* **2005**, *127*, 3635. (e) Huh, J. O.; Do, Y.; Lee, M. H. *Organometallics* **2008**, *27*, 1022. (f) Chiu, C.-W.; Kim, Y.; Gabbai, F. P. *J. Am. Chem. Soc.* **2009**, *131*, 60. (g) Chiu, C.-W.; Gabbai, F. P. *Dalton Trans.* **2008**, 814. (h) Agou, T.; Sekine, M.; Kobayashi, J.; Kawashima, T. *Chem.—Eur. J.* **2009**, *15*, 5056.

SCHEME 3. Plausible Mechanism of the Dual Emissions in 9[a]

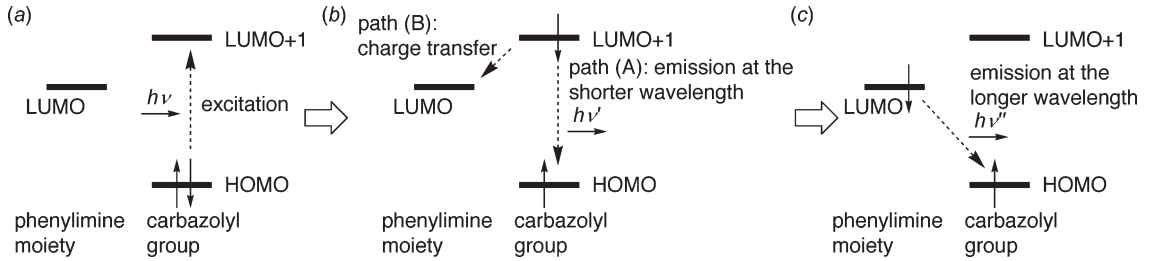

[a](a) At the absorption step. (b) At the relaxation step from the carbazolyl-group-localized excited state. (c) At the final emission step.

SCHEME 4. Reactions of 4a and 4c with NaCN

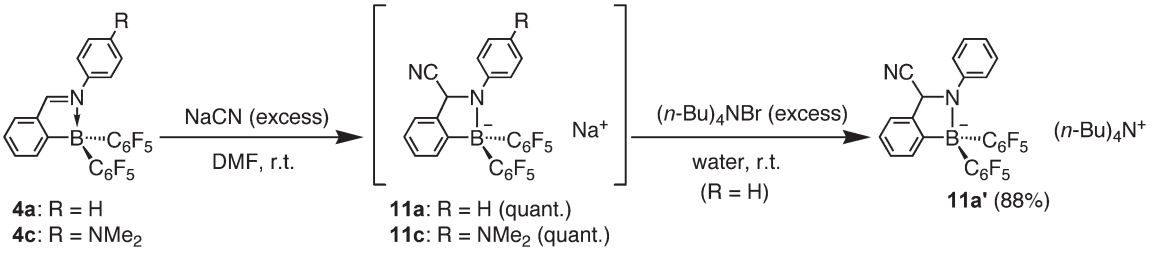

4a: R = H
4c: R = NMe_2

11a: R = H (quant.)
11c: R = NMe_2 (quant.)

11a' (88%)

shift of the absorption maxima suggests disconnection of the π-conjugated system of imine **4c**, meaning the formation of the corresponding cyanide adduct **11c** (Scheme 4). In the fluorescence spectra of the same solution, the emission of **4c** was completely quenched synchronically to the change in the absorption spectra (see Figure 12).

In the ^{19}F NMR spectra, two nonequivalent C_6F_5 groups of the products from **4a** and **4c** were observed. In the ^{13}C NMR spectra of the reaction solution of **4a**, the aldimine carbon signal (172.21 ppm) disappeared and new signals of a tertiary carbon (56.76 ppm) and a quaternary carbon (121.16 ppm) appeared instead (see Supporting Information). Finally, the cyanide adduct salt **11a′** was isolated in 88% yield by exchange of a countercation of **11a** with tetrabutylammonium bromide in water (Scheme 4) and fully characterized by spectroscopic methods and elemental analysis. These results clearly showed that the imine double-bond moiety of the fluorescent imines was a more favored site for reaction with a cyanide ion rather than the boron center. These results show that the imine C=N double bond is essential to the fluorescence of imines **4a** and **4c** and that changing the C=N double bond into the C−N single bond by addition of a cyanide ion can turn off their fluorescence. It is suggested that these 2-[bis(pentafluorophenyl)boryl]benzylideneamine derivatives, which do not release the toxic cyanide ion after binding, can be utilized as a cyanide ion sensor in the future.

Conclusion

Several boron-substituted imine derivatives, *N*-substituted 2-[bis(pentafluorophenyl)boryl]benzylideneamines, were synthesized very easily and in high yields by condensation of the corresponding formyl derivative and amines. In the boryl-substituted *N*-aryl and *N*-alkylimines, the B−N interaction provided them with fluorescence. Thus, nonfluorescent *N*-benzylideneaniline was converted into a blue-fluorescent material. The DFT and TD-DFT calculations showed that the B−N interaction raised the energy level of the $^3(n, \pi^*)$ excited state of the imine, resulting in suppression of the nonradiative deactivation via triplet states and hence fluorescence emission. Imines containing a more extended π-conjugated system and/or an electron-donating group on the π-system showed fluorescence that was more red-shifted with higher fluorescence efficiency. In the *N*-amino derivatives, dual emissions were observed. This phenomenon is explained as a result of the moderately perpendicular structure of the imine moieties. These findings concerning the relationship between structures and properties, especially fluorescence, in the fluorescent imine derivatives will expand the possibilities of utilizing imines as more versatile light-emitting devices. The dual emissions of hydrazones based on this new design can be applied to single-component white color emission material by further tuning of the substituents. Changing the fluorescence property of the *N*-arylimines by the formation of cyanide adducts showed that these 2-[bis(pentafluorophenyl)boryl]benzylideneamine derivatives have potential as a cyanide ion sensor in future investigations.

Experimental Section

Synthesis of (2-Formylphenyl)bis(pentafluorophenyl)borane (3). *n*-BuLi (1.5 M in hexane, 7.3 mL, 11 mmol) was added to an Et_2O solution (40 mL) of 2-bromobenzaldehyde diethyl acetal (2.20 mL, 10.9 mmol) at −78 °C. The reaction mixture was stirred for 1.5 h, added to an Et_2O solution (10 mL) of ethoxyborane **2** (3.00 mL, 11.4 mmol) at −78 °C, and allowed to warm gradually to rt. The reaction mixture was treated with water at rt and then with diluted hydrochloric acid, stirred for 1 h, and extracted with Et_2O. The organic layer was dried over anhydrous magnesium sulfate and evaporated. Recrystallization of the residue from Et_2O/hexane afforded **3** (2.45 g, 50%): pale brown crystals (Et_2O/hexane), mp 138.5−140.6 °C (dec). ^1H NMR (400 MHz, $CDCl_3$) δ 7.55 (t, ^3J = 7.6 Hz, 1H), 7.87 (t, ^3J = 7.6 Hz, 1H), 8.13−8.19 (m, 2H), 9.84 (s, 1H). ^{11}B NMR (128 MHz, $CDCl_3$) δ 8.5 (line width $h_{1/2}$ = 169 Hz). $^{13}C\{^1H\}$ NMR (100 MHz, $CDCl_3$) δ 114.0 (br s, *C*), 128.5 (s, *C*H), 130.3

(s, *C*H), 132.0 (quint, $^5J_{CF}$ = 3.3 Hz, *C*H), 135.6−138.57 (m, *C*), 138.64−141.7 (m, *C*), 139.0 (s, *C*H), 146.2−149.1 (m, *C*), 171.3 (br s, *C*), 201.2 (s, *C*H). A signal due to the carbon attached to the formyl group could not be detected. ^{19}F NMR (376 MHz, $CDCl_3$) δ −162.99 to −162.80 (m. 4F), −156.01 (t, $^3J_{FF}$ = 20 Hz, 2F), −132.05 to −131.90 (m, 4F). Anal. Calcd for $C_{19}H_5BF_{10}O$: C, 50.71; H, 1.12. Found: C, 50.85; H, 1.28%.

Typical Procedure for the Synthesis of {2-[Bis(pentafluorophenyl)boryl]benzylidene}amine Derivatives 4a−c and 5−9. A toluene (25 mL) solution of **3** (205 mg, 0.454 mmol) and aniline (42.4 mg, 0.455 mmol) was refluxed for 4 h, during which water generated in the reaction was removed with molecular sieves 4Å using a Soxhlet extractor. Evaporation of the solvent gave **4a** quantitatively. Recrystallization from benzene/hexane gave **4a** (199 mg, 83%): yellow crystals (benzene/hexane), mp 191.7−195.5 °C (dec). ^{1}H NMR (400 MHz, $CDCl_3$) δ 7.34−7.47 (m, 6H), 7.54 (ddd, ^3J = 7.6 Hz, ^3J = 7.3 Hz, ^4J = 0.7 Hz, 1H), 7.67 (d, ^3J = 7.3 Hz, 1H), 7.86 (d, ^3J = 7.6 Hz, 1H), 9.04 (s, 1H). ^{11}B NMR (128 MHz, $CDCl_3$) δ −1.8 (line width $h_{1/2}$ = 152 Hz). ^{13}C{^{1}H} NMR (100 MHz, $CDCl_3$) δ 115.8 (br s, *C*), 121.8 (s, *C*H), 127.2 (s, *C*H), 127.8 (s, *C*H), 128.6 (s, *C*H), 129.4 (s, *C*H), 129.7 (s, *C*H), 134.7 (s, *C*H), 135.5−141.1 (m, *C*, two signals overlapped each other), 136.6 (s, *C*), 140.9 (s, *C*), 146.4−149.3 (m, *C*), 165.8 (br s, *C*), 167.6 (s, *C*H). ^{19}F NMR (376 MHz, $CDCl_3$) δ −162.98 to −162.79 (m, 4F), −157.05 (t, $^3J_{FF}$ = 20 Hz, 2F), −131.68 to −131.52 (m, 4F). MS (EI, 70 eV) *m*/*z* 525 (37, M^+), 506 (21), 376 (24), 358 (100), 328 (31), 309 (65), 237 (69), 210 (63), 77(57), 51 (24%). UV−vis (hexane) λ_{max} (ε) 215 (1.4 × 10^4), 324 nm (1.0 × 10^4). Anal. Calcd for $C_{25}H_{10}BF_{10}N$: C, 57.18; H, 1.92; N, 2.67. Found: C, 57.07; H, 2.15; N, 2.59%.

Reaction of 4a with Sodium Cyanide. To a DMF solution (0.5 mL) of **4a** (47.6 mg, 90.6 μmol) in an NMR tube with a sealed tube of $CDCl_3$ for NMR locking was added sodium cyanide (5.2 mg, 0.11 mmol), and the mixture was shaken to make it homogeneous. Disappearance of **4a** and quantitative formation of cyanide adduct **11a** were observed by ^{11}B, ^{13}C, and ^{19}F NMR spectroscopy. **11a**: ^{11}B NMR (128 MHz, DMF) δ −4.5 (line width $h_{1/2}$ = 81 Hz). ^{13}C{^{1}H} NMR (126 MHz, DMF) δ 56.8 (s, *C*H), 114.6 (s, *C*H), 114.7 (s, *C*H), 121.2 (s, *C*), 122.4 (s, *C*H), 126.1 (s, *C*H), 126.4 (br s, *C*), 128.1 (s, *C*H), 128.65 (s, *C*H), 128.73 (s, *C*H), 135.0−139.8 (m, two signals overlapped each other, *C*), 140.9 (s, *C*), 146.7−150.3 (m, two signals overlapped each other, *C*), 149.7 (s, *C*), 156.2 (br, *C*). ^{19}F NMR (376 MHz, DMF) δ −166.47 to −166.24 (m, 2F), −166.81 to −166.59 (m, 2F), −163.16 (t, $^3J_{FF}$ = 20 Hz, 1F), −162.61 (t, $^3J_{FF}$ = 20 Hz, 1F), −133.30 (br s, 2F), −133.00 (d, $^3J_{FF}$ = 18 Hz, 2F).

Reaction of 4c with Sodium Cyanide. Similarly, the reaction of **4c** (4.5 mg, 7.9 μmol) with sodium cyanide (29 mg, 0.59 mmol) in DMF (1.0 mL) gave observation of disappearance of **4c** and quantitative formation of cyanide adduct **11c** in ^{11}B and ^{19}F NMR. **11c**: ^{11}B NMR (128 MHz, DMF) δ −4.4 (line width $h_{1/2}$ = 80 Hz). ^{19}F NMR (376 MHz, DMF) δ −166.84 to −166.64 (m, 2F), −166.53 to −166.32 (m, 2F), −163.39 (t, $^3J_{FF}$ = 20 Hz, 1F), −162.76 (t, $^3J_{FF}$ = 20 Hz, 1F), −133.64 to −132.74 (m, 4F). UV−vis (DMF) λ (ε) 302 (1.6 × 10^4), 328 nm (1.2 × 10^4).

Isolation of Tetrabutylammonium Salt of a Cyanide Adduct of 4a. A DMF solution (1.0 mL) of **4a** (101 mg, 0.192 mmol) was added to sodium cyanide (52.7 mg, 1.08 mmol) at rt. The reaction mixture was stirred for 30 min, treated with aqueous solution (100 mL) of tetrabutylammonium bromide (517 mg, 1.60 mmol), and stirred for additional 10 min. Filtration of the precipitate followed by washing with water afforded **11a′** (134 mg, 88%): colorless solid (DMF/water), mp 51.2−62.8 °C (dec). ^{1}H NMR (400 MHz, $CDCl_3$) δ 0.92 (t, ^3J = 7.3 Hz, 12H), 1.27 (sext, ^3J = 7.3 Hz, 8H), 1.36−1.47 (m, 8H), 2.80−2.88 (m, 8H), 5.76 (s, 1H), 6.45 (t, ^3J = 7.1 Hz, 1H), 6.75 (d, ^3J = 8.1 Hz, 2H), 7.01−7.06 (m, 2H), 7.15−7.18 (m, 2H), 7.37−7.41 (m, 1H), 7.50−7.54 (m, 1H). ^{11}B NMR (128 MHz, $CDCl_3$) δ −4.9 (line width $h_{1/2}$ = 125 Hz). ^{13}C{^{1}H} NMR (126 MHz, $CDCl_3$) δ 13.4 (s, *C*H$_3$), 19.5 (s, *C*H$_2$), 23.6 (s, *C*H$_2$), 56.4 (s, *C*H), 58.3 (s, *C*H$_2$), 113.7 (s, *C*H), 114.2 (s, *C*H), 121.4 (s, *C*), 121.6 (s, *C*H), 125.4 (s, *C*H), 127.7 (s, *C*H), 128.3 (s, *C*H), 128.7 (s, *C*H), 135.1−139.9 (m, two signals overlapped each other, *C*), 139.4 (s, *C*), 146.5−149.9 (m, two signals overlapped each other, *C*), 149.3 (s, *C*), 156.4 (br, *C*). A signal due to the carbon attached to the boron could not be detected. ^{19}F NMR (376 MHz, $CDCl_3$) δ −166.14 to −165.72 (m, 4F), −162.96 (t, $^3J_{FF}$ = 22 Hz, 1F), −161.72 (t, $^3J_{FF}$ = 20 Hz, 1F), −134.77 to −133.27 (m, 4F). MS (FAB$^+$) *m*/*z* 242 (Bu_4N^+). MS (FAB$^-$) *m*/*z* 551 ([M − Bu_4N]$^-$). UV−vis (THF) λ (ε) 257 (1.1 × 10^4), 278 nm (1.3 × 10^4). Anal. Calcd for $C_{42}H_{46}BF_{10}N_3$: C, 63.56; H, 5.84; N, 5.29. Found: C, 63.35; H, 5.82; N, 5.14%.

X-ray Crystallographic Analysis. X-ray diffraction data for single crystals of **4a−c** and **5−9** were collected using Rigaku MERCURY CCD. The structures were solved by the direct method and refined by full-matrix least-squares using SHELX-97.[18]

Theoretical Calculations. All calculations were carried out at the DFT level using the B3PW91[19,20] exchange-correlation functional implemented in the Gaussian 03 (Revision D.02)[21] suite of programs. All calculations were performed with the 6-31+G(d) basis set. The energy levels of excited states were obtained by a time-dependent DFT (TD-DFT) method. Zero point energy corrections are not included in all the calculations.

Acknowledgment. We thank Dr. Tomohisa Takaya and Mr. Hiroaki Itoi (The University of Tokyo, Japan) for their measurement of fluorescence lifetimes. We thank Tosoh Finechem Corp. and Central Glass Co., Ltd. for gifts of alkyllithiums and fluorine compounds, respectively. This work was partially supported by Grants-in-Aid for the Global COE Program for Chemistry Innovation and for Scientific Researches from the Ministry of Education, Culture, Sports, Science and Technology, Japan and the Japan Society for the Promotion of Science. J.Y. was granted a Research Fellowship of Japan Society for the Promotion of Science for Young Scientists. N.K. thanks Shorai Foundation for Science and Technology, Iketani Science and Technology Foundation, and Mistubishi Chemical Corporation for research grants.

Supporting Information Available: General experimental methods. Compound characterization data for **4b**, **4c**, and **5−9**. Crystal data for **4a−c** and **5−9**. ORTEP drawings of **4a−c** and **5−9**. A part of the packing structures of **8** in the unit cell. Cartesian coordinations of optimized structures by DFT calculations. Full list of authors for ref 21. NMR spectra of new compounds. Crystallographic data in CIF format. This material is available free of charge via the Internet at http://pubs.acs.org.

(18) Sheldrick, G. M., *SHELX-97*, University of Göttingen: Göttingen, Germany, 1997.
(19) Becke, A. D. *J. Chem. Phys.* **1993**, *98*, 5648.
(20) Pardew, J. P.; Bruke, K.; Wang, Y. *Phys. Rev. B* **1996**, *54*, 16533.
(21) Frisch, M. J. et al. *Gaussian 03*, revision D.02; Gaussian, Inc.: Wallingford, CT, 2004.